How to Cite:
Shervegar, V. M. (2022). Phonocardiogram event-based delineation method using continuous wavelet transform. *International Journal of Health Sciences*, *6*(S4), 4039–4054. https://doi.org/10.53730/ijhs.v6nS4.9032

Phonocardiogram event-based delineation method using continuous wavelet transform

Dr. Vishwanath Madhava Shervegar
Associate Professor, Mangalore Institute of Technology and Engineering, Moodbidri, Dakshina Kannada, Karnataka, India
Corresponding author email: vishwanath@mite.ac.in

***Abstract*---**Objective: This paper represents a new method of Phonocardiogram delineation using the heart sound events extracted from the Continuous Wavelet transformation of the Phonocardiogram. Methods: The Phonocardiogram signals were filtered using the Chebyshev bandpass Type-II filter to remove the noise. A two-dimensional Time-Frequency Continuous Wavelet Transform operator was applied to the Phonocardiograms to convert the audio signal into the time-frequency Spectrogram. The Row sum of the Spectrogram matrix was evaluated by summing the matrix for all frequencies along with the time axis. The average of the row sum was calculated. This average value was then subtracted from the row sum. The intersection of the deduced row sum, after subtraction, indicated the boundaries of the Phonocardiogram. Beat identification in the Phonocardiogram was done using Fast Fourier Transform. Conclusion: The method can identify the boundaries of the sounds in the Phonocardiogram and indicate the presence of the First heart sound-systole-Second heart sound-diastole sequence with an accuracy of 90.1% and an F1 score of 94.8%. Significance: The method can be used to delineate Phonocardiograms without any external reference like ECG, PPG, or carotid Pulse. No additional signal processing overheads like noise threshold, activity detection, or feature extraction are involved.

***Keywords*---**Peter-Bentley PCG database, phonocardiogram, wavelets, event detection, noise threshold.

Introduction

The phonocardiogram (PCG) signal detects and records heart sounds, the sounds made by the various cardiac structures pulsing and moving blood [1]. This sound is caused usually by the acceleration and deceleration of blood and turbulence developed during the rapid blood flow [1]. An electronic stethoscope remains the primary technology of the doctor for hearing such sounds [2]. When an electronic

stethoscope is placed on the subject's chest, the first cardiac sound (S1) and the second cardiac sound (S2) are audible [2]. A stethoscope system consisting of an electronic stethoscope and a digital assistant like a smartphone or a laptop is used to assess the condition of the heart [2]. The digital assistant uses an application based on the various types of signal processing techniques that have been developed to analyze the condition of the heart [2]. The signal processing technique involved in dividing the cardiac sounds into S1-S2 and S2-S1 cycles is called segmentation [2]. Segmentation helps to assess the occurrence of cardiac events [2]. The most popular method of cardiac sounds is the wavelet transform [3,4]. Dinesh Kumar et al. performed segmentation of the cardiac sounds by using the wavelet decomposition simplicity filter [3,4]. In the early years, various threshold-based techniques based on Shannon Energy, S-transform, and Wavelet transform were used to segment the Phonocardiograms [5-12]. In the later years, statistical models based on HMM, HSMM, GMM, and SVM referred HSMM were used to segment the Phonocardiograms [13-17]. Of late, classifier-based methods using SVM, ANN, CNN, and deep neural networks have been used to segment Phonocardiograms with good accuracy [18-22]. One of the main drawbacks of the classifier-based methods is their reliance on the feature extraction or activity detection mechanism which is required for PCG delineation [22]. We have developed a simple Spectrogram based method involving a 2D-Continuous Wavelet Transform (CWT) that can detect the boundaries of the cardiac events. Fast Fourier transform has been utilized to identify the beats. No additional signal processing overheads like noise threshold, activity detection, or feature extraction are involved.

Segmentation of Phonocardiograms

The segmentation of PCG signal using CWT is divided into 5 steps namely preprocessing, CWT computation, evaluation of wavelet energy, boundary extraction, and S1-systole-S2-diastole identification. Each of them is explained explicitly in the sections given below.

Preprocessing

The Phonocardiogram signal is first down-sampled from 44100 Hz to 441 Hz to reduce the sample size by 100 times. The sampled signal is further filtered using a Chebyshev Type II bandpass filter with a cut-off frequency of 20Hz-160Hz to remove most of the noise redundant in the signal. Filtering the signal removes unwanted perturbations and smoothens the signal. Fig 1 shows the original raw signal in pane 1 and the filtered signal in pane 2. Fig 2 shows the zoom plot of Fig 1.

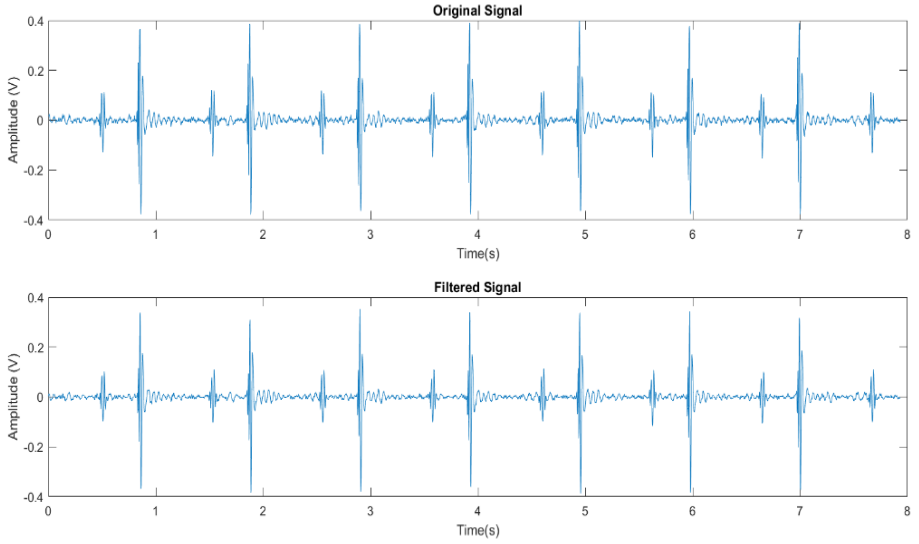

Fig 1 Original and Filtered PCG signal

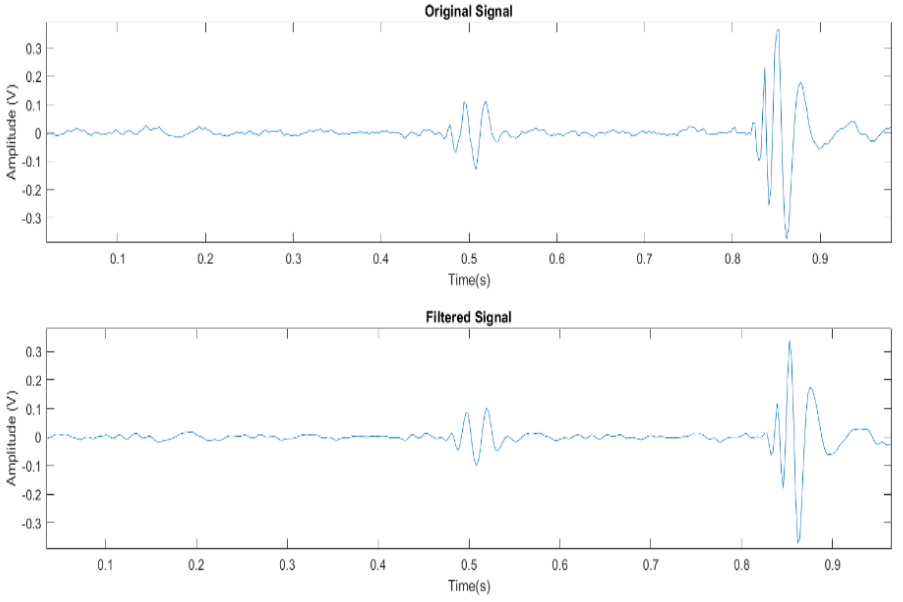

Fig 2 Original and Filtered PCG signal (zoom plot)

CWT Computation

The Continuous Wavelet transform of the filtered PCG signal is then computed after removing the noise. Morlet wavelet is used as the mother wavelet for CWT computation. The Morlet wavelet was selected because of its morphological resemblance of the wavelet with the PCG signal. Matlab CWT function is used to

compute the Continuous wavelet transform. The CWT Coefficient matrix $\boldsymbol{C_M(a,b)}$was estimated as

$$\boldsymbol{C_M(a,b) = \int_{-\infty}^{\infty} x(t)\psi_{a.b}(t).} \quad (1)$$

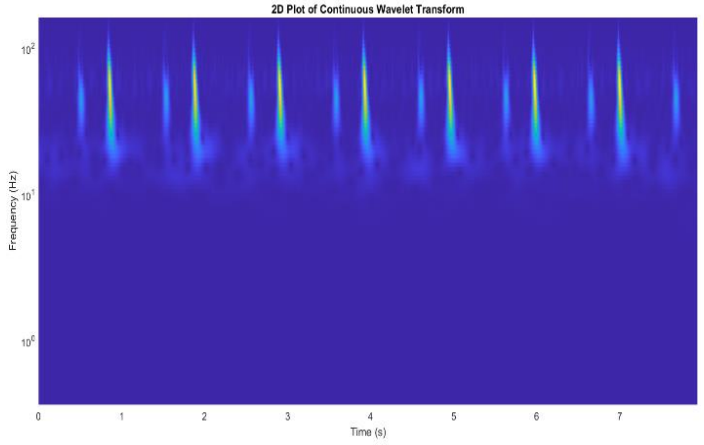

Fig 3 CWT Spectrogram

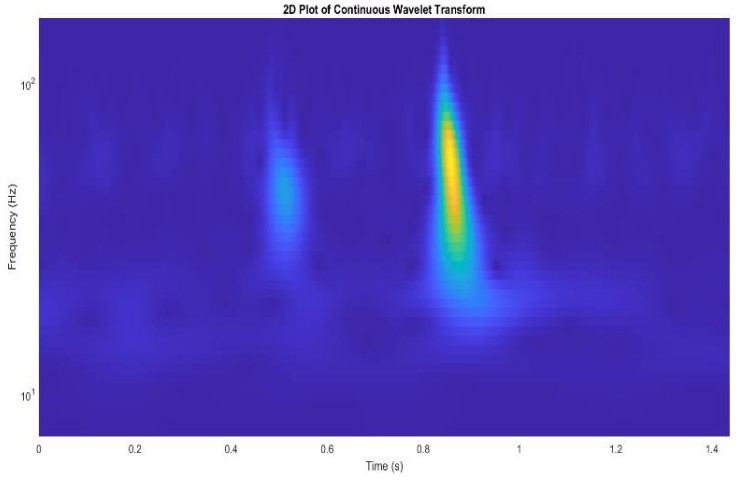

Fig 4 CWT Spectrogram (Zoomed Plot)

Where $\boldsymbol{x(t)}$ is the PCG and $\boldsymbol{\psi_{a.b}(t)}$ represents the mother wavelet (Morlet) with scale $\boldsymbol{a}$ dilation $\boldsymbol{b}$. Fig 3 represents the CWT spectrogram of the normal PCG signal. Fig 4 represents the zoomed plot.

Evaluation of Wavelet Energy

Evaluation of CWT coefficients of the filtered signal results in CWT matrix. The row sum of the CWT matrix is computed to obtain the wavelet energy. Fig 5 Pane 1 indicates the wavelet energy. The wavelet energy signal contains many sharp spikes. These spikes are smoothened using the moving average filter. The window

size of the filter is arbitrarily fixed at 10 to obtain optimum smoothness. The wavelet energy signal is computed as

$$\boldsymbol{W_E(t) = \sum C_M(a,b)} \qquad (2)$$

Where, $\boldsymbol{C_M(a,b)}$ represents the CWT coefficients. The wavelet energy signal is smoothened by the moving-average filter. The moving average filter is defined as

$$\boldsymbol{M_A = \frac{\sum W_E}{n}}. \qquad (3)$$

$\boldsymbol{W_E}$ represents the data points and $\boldsymbol{n}$ represents the total number of data points. Fig 5 Pane 2 indicated the wavelet energy signal after smoothening.

Boundary Extraction

After smoothening the signal in step 3 the mean value of the smoothened wavelet energy signal is computed. The mean value is then subtracted from the smoothened wavelet energy signal to obtain the corrected smoothened wavelet energy signal with a zero line as the reference axis. The zero crossings of the corrected smoothened wavelet energy signal with the zero-reference line are noted. The zero crossings indicate the boundaries of the sounds in the PCG signal.

S1-systole-S2- diastole identification

The Fast Fourier Transform of the sounds within the boundaries is computed. Generally, the first heart sound has frequency components in the range 30Hz-150Hz, while the second heart sound has frequency components in the range 200Hz-280Hz [22]. So, by using these metrics we have identified the heart sounds as S1-systole-S2-diastole. Fig 5 pane 3 shows the Segmented sounds in the smoothened wavelet energy signal. Fig 6 shows the zoomed plot. Fig 7 shows the original segmented PCG signal and Fig 8 shows the zoomed plot. The red color indicates the S1 sound while the pink color indicated the S2 sound as per sound identification done using Fast Fourier Transform.

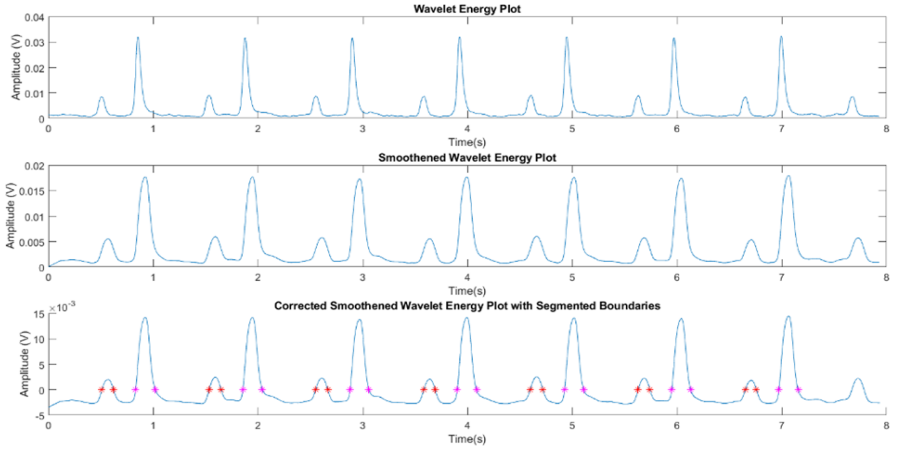

Fig 5 Wavelet Energy Signal

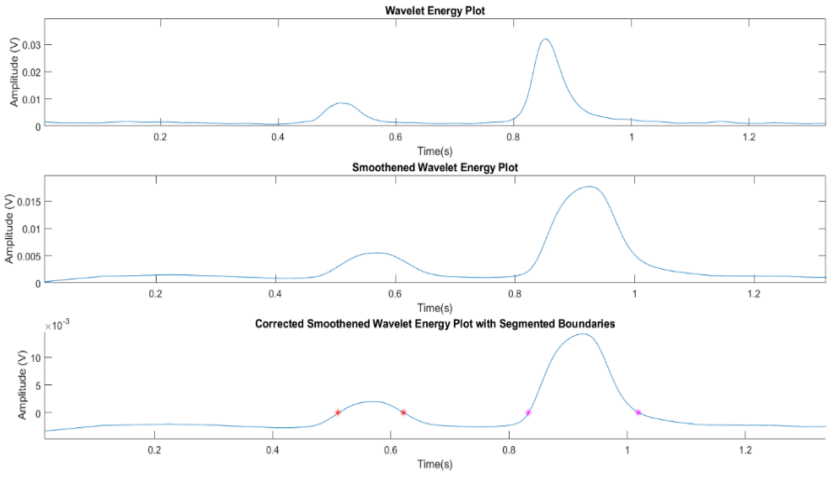

Fig 6 Wavelet Energy Signal (Zoom Plot)

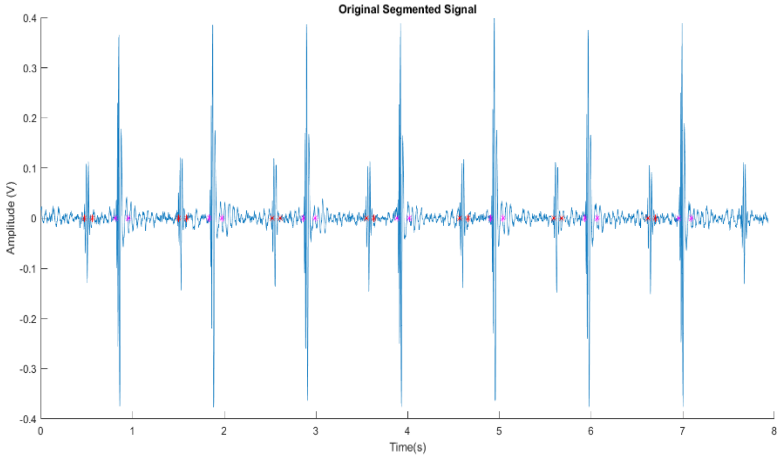

Fig 7 Segmented PCG Signal

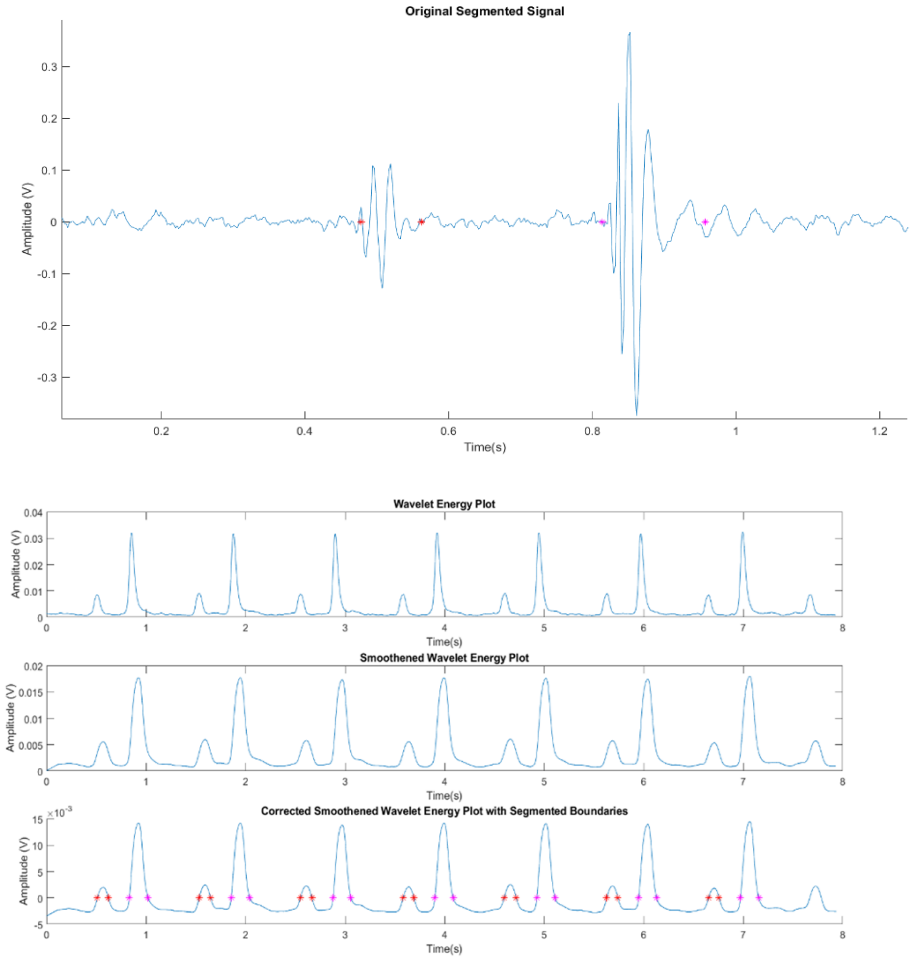

Fig 8 Segmented PCG Signal (zoomed plot)

Results and Discussion

This section describes the results obtained from applying the CWT-based segmentation on PCG signals from the Peter Bentley PCG database.

Dataset

Two datasets were provided for the Peter Bentley PCG segmentation challenge [23]. Dataset A comprises data crowd-sourced from the general public via the stethoscope Pro iPhone app [23]. Dataset B comprises data collected from a clinical trial in hospitals using the digital stethoscope Digi-Scope [23]. The audio files are of varying lengths, between 1 second and 30 seconds (some have been clipped to reduce excessive noise and provide the salient fragment of the sound). Most information in heart sounds is contained in the low-frequency components, with noise in the higher frequencies [23]. It is common to apply a low-pass filter at

160 Hz [23]. Fast Fourier transforms are also likely to provide useful information about volume and frequency over time [23].

Segmentation of PCG

The cardiac sounds are selected from the PCG Peter Bentley database. The PCG signals are first preprocessed by down-sampling 100 times from a sampling frequency of 44100 Hz to 441 Hz and then filtered by a Type II Chebyshev bandpass filter with a cut-off frequency of 20 Hz to 160 Hz. CWT segmentation procedure is then applied to the filtered sounds. In the segmentation procedure, the CWT matrix is computed first. Then the wavelet energy is found from the CWT matrix by taking the row-sum. The wavelet energy signal is smoothened by a moving-average filter with a window size fixed at 10. The mean value of the smoothened signal is then evaluated by taking the average of the samples. The mean value is then subtracted from the original smoothened signal to obtain the corrected smoothened wavelet energy signal. The zero-reference line of the corrected smoothened wavelet energy signal is used to extract the boundaries of the PCG. The zero crossings of the corrected smoothened wavelet energy signal are noted. The sounds within the boundary are either the first heart sound or the second heart sound. The Fast Fourier Transform is evaluated for the sounds within the boundary. Fast Fourier Transform is a plot of frequency versus wavelet energy. The sounds with a lesser frequency range are marked as the first heart sound while those with higher frequencies are marked as the second heart sound. We have effectively used Fast Fourier Transform for labeling the occurrence of S1-systole-S2-diastole in the PCG signal.

The segmentation algorithm is applied to both datasets A and B. Both the datasets have 4 categories of sounds namely Normal, Murmur, Extrasystole, and Artifact. Apart from that, they have a separate set of unlabeled sounds in datasets A and B. Fig 9 shows the original segmented normal PCG and the zoomed plot in Fig 10. The plot shows silence in the systole and diastole. Fig 11 shows the original segmented diastolic murmur PCG and its zoom plot in Fig 12. The murmur sounds are visible in the diastole. Fig 13 shows the original segmented Extrasystole PCG and its zoom plot in Fig 14. The extra sounds are visible here that corresponds to clicks and snaps. Fig 15 and zoomed plot Fig 16 shows the unlabeled PCG signal with its heart sound components. The figure shows a large S1 sound with a small S2 sound.

Tables 1-6 give the split-up of the metrics obtained by applying the segmentation algorithm. All together 643 PCG signals were involved of which 134 signals were from dataset A while the remaining 509 signals were from dataset B. Ten percent of the signals were rejected due to the presence of high noise and murmurs which could not be removed even after filtering. Out of the retained 580 PCG signals, 121 signals were considered from dataset A while 459 signals were considered from dataset B. Both dataset A and dataset B have signals under the category of Normal, Murmur, Extrasystole, and Unlabeled sounds. In dataset A, the segmentation procedure yielded 909 true positive S1 and S2 sounds from all categories. 62 sounds were categorized as false positives due to bad segmentation. 28 sounds were categorized as false negatives with no segmentation. In dataset B, segmentation procedure yielded 4182 true positive S1 and S2 sounds from all

categories. 349 sounds were categorized as false positives due to bad segmentation. 118 sounds were categorized as false negatives with no segmentation. Considering the full database of sounds, segmentation procedure yielded 5091 true positive S1 and S2 sounds from all categories. 411 sounds were categorized as false positives due to bad segmentation. 146 sounds were categorized as false negatives with no segmentation.

Sounds	TP	FP	FN
Normal	213	15	5
Murmur	331	10	11
Extrasystole	74	20	1
Unlabeled	291	17	11
Total	909	62	28

Table 1 True Positive, False Positive and False Negative of the various PCG sounds (dataset A)

Sounds	Accuracy (Ac)	Positive Predictive Value (P_+)	Sensitivity (Se)	F1 measure
Normal	91.4	93.4	97.7	95.5
Murmur	94.0	97.1	96.8	96.9
Extrasystole	77.9	78.7	98.7	87.6
Unlabeled	91.2	94.5	96.4	95.4
Total	90.9	93.6	97.0	95.3

Table 2 PCG signal (dataset A) Metrics (Accuracy, Positive Predictive Value, Sensitivity and F1 Measure)

Sounds	TP	FP	FN
Normal	2223	78	75
Murmur	273	48	1
Extrasystole	459	88	13
Unlabeled	1227	135	29
Total	4182	349	118

Table 3 True Positive, False Positive and False Negative of the various PCG sounds (dataset B)

Sounds	Accuracy (Ac)	Positive Predictive Value (P_+)	Sensitivity (Se)	F1 measure
Normal	93.6	96.7	96.6	96.6
Murmur	84.8	85	99.6	91.7
Extrasystole	81.9	83.9	97.2	90
Unlabeled	88.2	90	97.7	94.8
Total	90	92.3	97.3	94.7

Table 4 PCG signal (dataset B) Metrics (Accuracy, Positive Predictive Value, Sensitivity and F1 Measure)

Sounds	TP	FP	FN
Normal	2436	93	80

Murmur	604	58	12
Extrasystole	533	108	14
Unlabeled	1518	152	40
Total	5091	411	146

Table 5 True Positive, False Positive and False Negative of the various PCG sounds (overall dataset)

Sounds	Accuracy (Ac)	Positive Predictive Value (P_+)	Sensitivity (Se)	F1 measure
Normal	93.4	96.3	96.8	96.5
Murmur	89.6	83.2	97.4	89.7
Extrasystole	81.4	91.2	98	94.5
Unlabeled	88.8	90.0	97.4	93.6
Total	90.1	92.5	97.2	94.8

Table 6 PCG signal (overall dataset) Metrics (Accuracy, Positive Predictive Value, Sensitivity and F1 Measure)

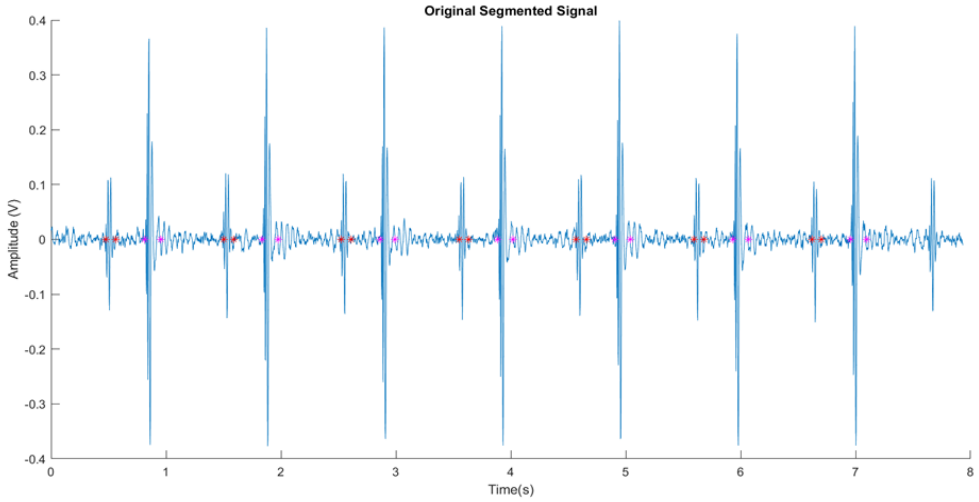

Fig 9 Segmented Normal PCG Signal

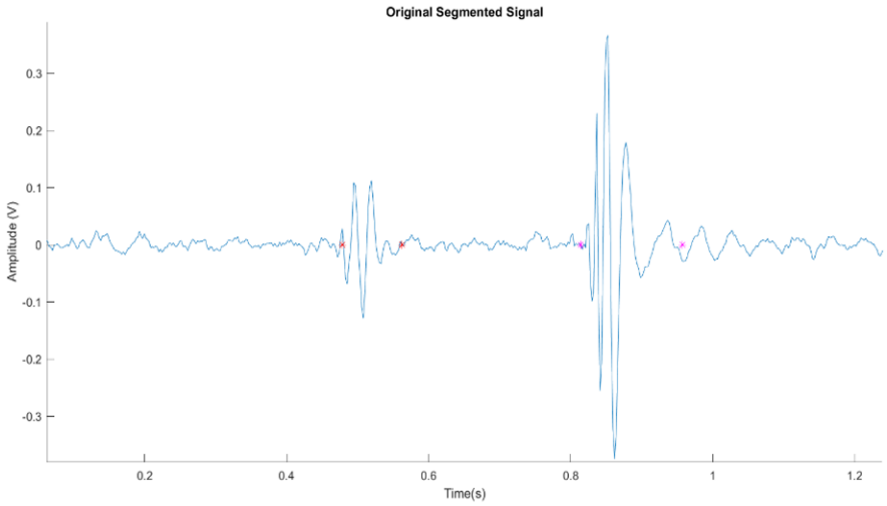

Fig 10 Segmented Normal PCG Signal (zoomed plot)

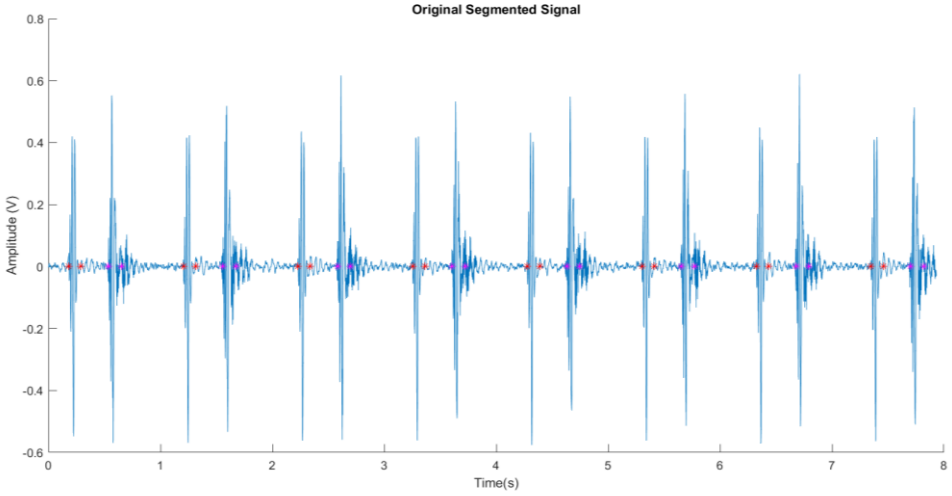

Fig 11 Segmented Diastolic Murmur PCG Signal

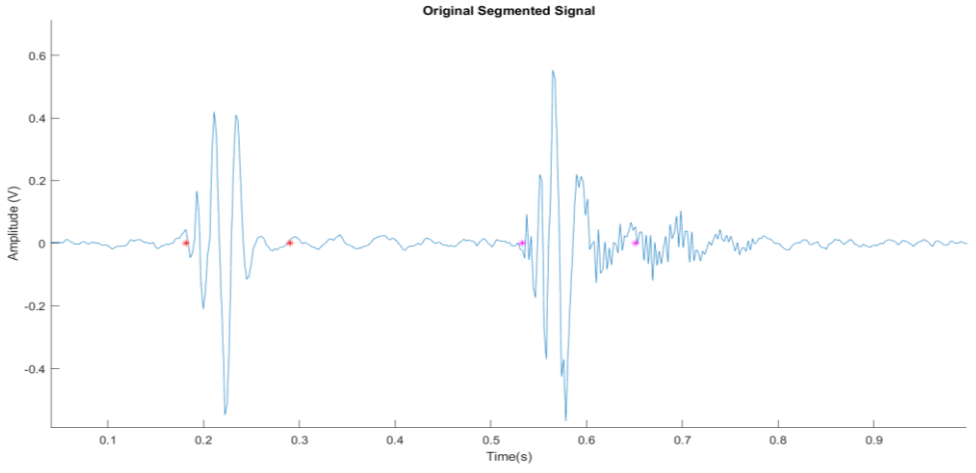

Fig 12 Segmented Diastolic Murmur PCG Signal (zoomed plot)

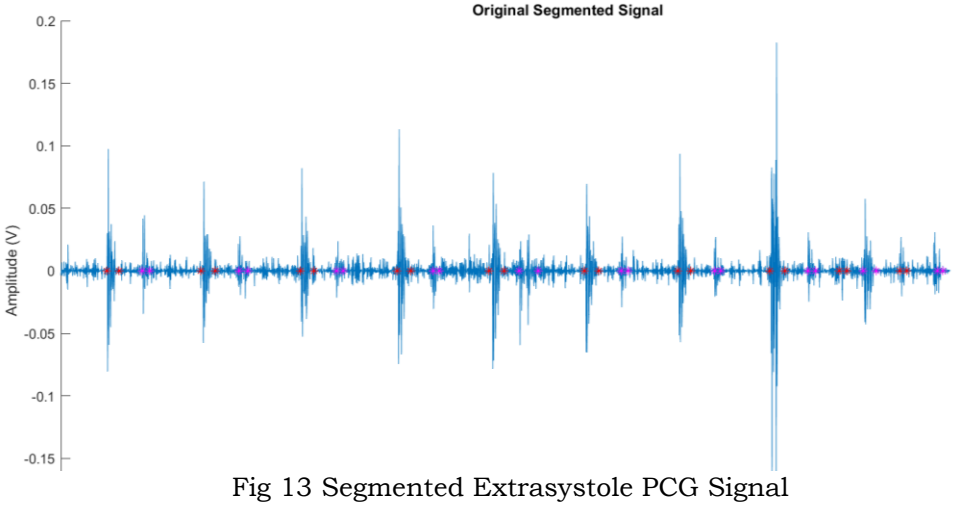

Fig 13 Segmented Extrasystole PCG Signal

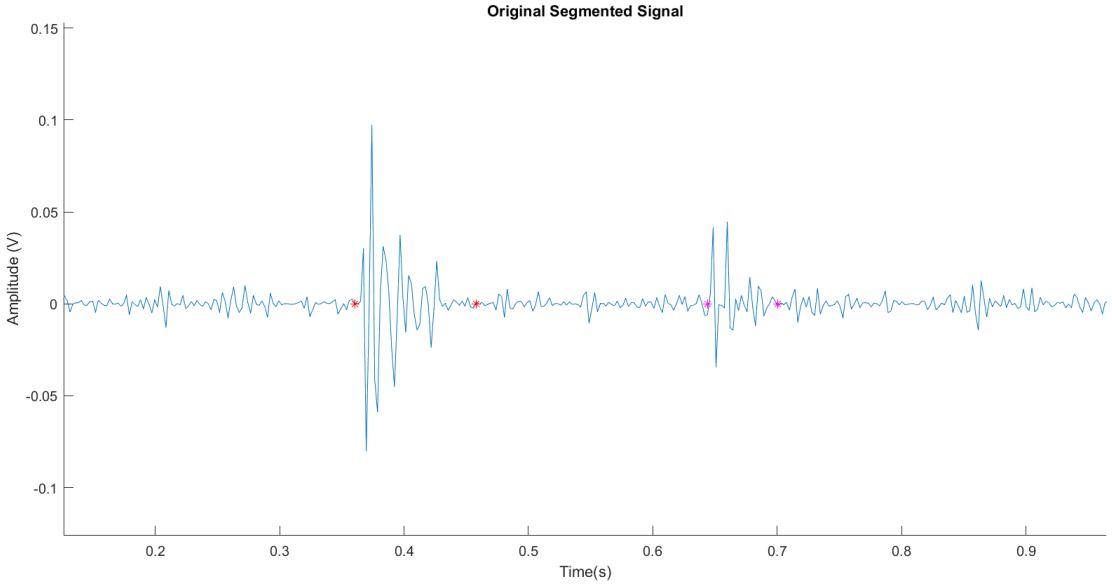

Fig 14 Segmented Extrasystole PCG Signal (zoomed plot)

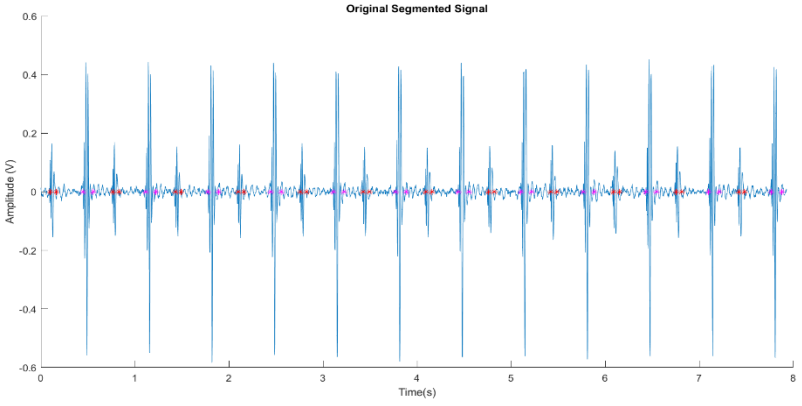

Fig 15 Segmented Unlabeled PCG Signal

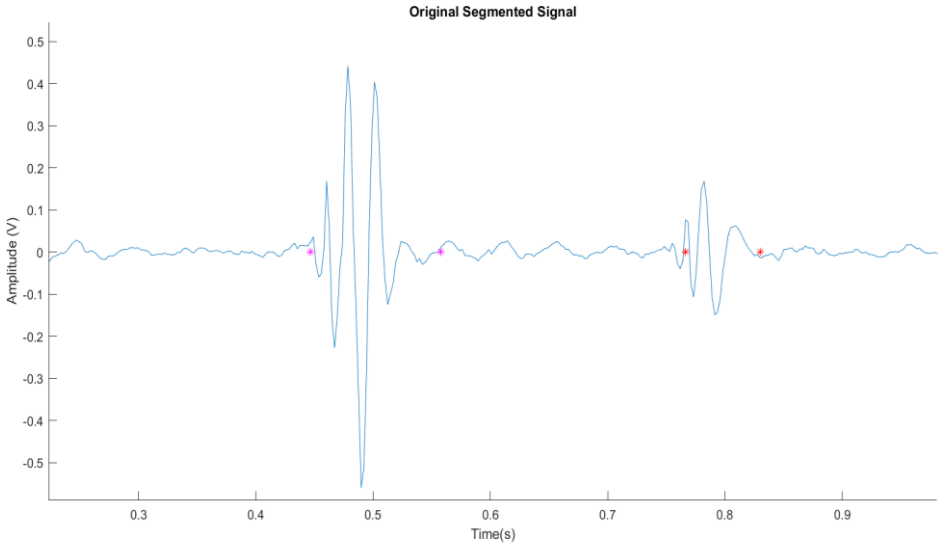

Fig 16 Segmented Unlabeled PCG Signal (zoomed plot)

Conclusion

From the above results and discussion, it is evident that the PCG signal can be segmented by the CWT technique. We have achieved an accuracy of 90.1% and an F1 score of 94.8%. for both the datasets A and B. This segmentation procedure is a simple technique that involves no overheads like noise threshold, activity detection or feature extraction. The technique can be incorporated into the stethoscope system connected to a laptop or a smartphone. The computational efficiency is high and the cost of implementation is low.

Conflicts of Interest: None
Funding: None
Ethical Approval: Not required

References

1. Gerald Goodman, “Clinical Engineering Handbook”, Elsevier, 2004.
2. Shervegar et al., “Automatic segmentation of Phonocardiogram using the occurrence of the cardiac events”, Informatics in Medicine Unlocked, Elsevier, Vol 9, No 1, 2017.
3. Gupta CN, Palaniappan R, Swaminathan S, Krishnan SM. Neural network classification of homomorphic segmented heart sounds. Appl Soft Comput 2007; 7:286–97.
4. Kumar D, Carvalho P, Antunes M, Henriques J, Maldonado M, Schmidt R, et al., “Wavelet transform and simplicity-based heart murmur segmentation”, Computing in Cardiology, 2006;33:173–6.
5. H.Liang et al., “Heart sound segmentation algorithm based on heart sound envelogram,” in Proc. Comput. Cardiol., Lund, Sweden, 1997, vol. 24, pp. 105–108.

6. H. Liang et al., “A heart sound segmentation algorithm using wavelet decomposition and reconstruction,” in Proc. 19th Annu. Int. Conf. IEEE Eng. Med. Biol. Soc., Chicago, IL, USA, 1997, vol. 4, pp. 1630–1633.
7. D. Kumar et al., “Detection of S1 and S2 heart sounds by high-frequency signatures.” in Proc. 28th Annu. Int. Conf. IEEE Eng. Med. Biol. Soc., New York, NY, USA, 2006, vol. 1, pp. 1410–1416.
8. S.Ariet al., “A robust heart sound segmentation algorithm for commonly occurring heart valve diseases.” J. Med. Eng. Technol., vol. 32, no. 6, pp. 456–65, Jan. 2008.
9. J. Vepa et al., “Segmentation of heart sound using simplicity features and timing information,” in Proc. IEEE Int. Conf. Acoust., Speech Signal Process., Las Vegas, NV, USA, 2008, pp. 469–472.
10. C.Gupta et al., “Neural network classification of homomorphic segmented heart sound,” Appl. Soft Comput., vol. 7, no. 1, pp. 286–297, Jan. 2007.
11. T. Chen et al., “Intelligent heart sound diagnostics on a cellphone using a hands-free kit,” in Proc. AAAI Spring Symp. Artif. Intell. Dev., Stanford University, Stanford, CA, USA, 2010, pp. 26–31.
12. T. Oskiper and R. Watrous, “Detection of the first heart sound using a time-delay neural network,” in Proc. IEEE Comput. Cardiol., Memphis, TN, USA, 2002, pp. 537–540.
13. D. Gill, N. Gavrieli, and N. Intrator, “Detection and identification of heart sound using homomorphic envelogram and self-organizing probabilistic model,” in Computers in Cardiology, 2005, pp. 957–960.
14. Y.-J. Chung, Pattern Recognition and Image Analysis, Iberian Conference. Berlin, Heidelberg: Springer Berlin Heidelberg, 2007, Classification of Continuous Heart Sound Signals Using the Ergodic Hidden Markov Model, pp. 563–570.
15. S. Schmidt, C. Holst-Hansen, C. Graff, E. Toft, and J. J. Struijk, “Segmentation of heart sound recordings by a duration-dependent hidden Markov model,” Physiological measurement, vol. 31, no. 4, pp. 513–529, 2010.
16. D. B. Springer, L. Tarassenko, and G. D. Clifford, “Support vector machine hidden semi-Markov model-based heart sound segmentation,” In Computing in Cardiology Conference (CinC), 2014, Sept 2014, pp.625–628.
17. Springer et al., “Logistic regression-HSMM-based heart sound segmentation,” IEEE Trans. Biomed. Eng., vol. 63, no. 4, pp. 822–832, 2016.
18. J. Vepa, “Classification of heart murmurs using cepstral features and support vector machines,” in IEEE EMBC, 2009, pp. 2539–2542.
19. T. Leung, P. White, W. Collis, E. Brown, and A. Salmon, “Classification of heart sounds using time-frequency method and artificial neural networks,” in IEEE EMBC, 2000, pp. 988–991.
20. T.-E. Chen, S.-I. Yang, L.-T. Ho, K.-H. Tsai, Y.-H. Chen, Y.-F. Chang, Y.-H. Lai, S.-S. Wang, Y. Tsao, and C.-C. Wu, “S1 and S2 heart sound recognition using deep neural networks,” IEEE Trans. Biomed. Eng., vol. 64, no. 2, pp. 372–380, 2017.
21. Francesco Renna, Jorge Oliveira, Miguel T. Coimbra, “Convolutional Neural Networks for Heart Sound Segmentation”, European Signal Processing Conference (EUSIPCO 2018).
22. Brusco and Nazarene, “Digital Phonocardiography-A PDA based approach”, Annual International Conference of the IEEE Engineering in Medicine and

Biology Society. IEEE Engineering in Medicine and Biology Society. Conference 3:2299-302, 2004.
23. Website of PCG database (Accessed 08th April 2022): www.peterjbentley.com.
24. Rinartha, K., & Suryasa, W. (2017). Comparative study for better result on query suggestion of article searching with MySQL pattern matching and Jaccard similarity. In *2017 5th International Conference on Cyber and IT Service Management (CITSM)* (pp. 1-4). IEEE.
25. Rinartha, K., Suryasa, W., & Kartika, L. G. S. (2018). Comparative Analysis of String Similarity on Dynamic Query Suggestions. In *2018 Electrical Power, Electronics, Communications, Controls and Informatics Seminar (EECCIS)* (pp. 399-404). IEEE.